

Bromine-Sensitized Solar Photolysis of CO₂

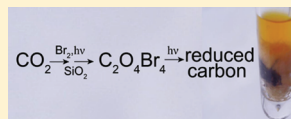
Mark S. Braiman,* Wilfried Sailer-Kronlachner, and Christopher J. Varjas

Chemistry Department, Syracuse University, Syracuse, New York 13244, United States

S Supporting Information

ABSTRACT: Direct photochemical reduction of CO₂ has generally been accomplished by using transition-metal compounds as electron transfer reagents. Here, we show that elemental bromine can function as an alternative photosensitizer. When sunlight is tightly focused on mixtures of CO₂ and Br₂, in the presence of a polar adsorbent such as silica gel, glass wool, alumina, or titania, a metastable red adduct is formed within seconds and concentrates at the point of illumination.

Further illumination causes deposition of a stable black film on the polar adsorbent. Mass spectrometry of the cold-trapped red intermediate shows clusters of peaks corresponding to the expected distribution of isotopomers of C₂O₄Br₄⁺, as well as of C₂O₄Br₃⁺. DFT computations indicate that the lowest-energy species with the formula C₂O₄Br₄ is trans-2,4-dibromo-2,4-dihypobromo-1,3-dioxetane. Formation of this molecule from (2CO₂ + 2Br₂) would require a minimum of 3 visible photons, two of which would hypothetically be used in formation of as-yet undetected CO₂Br₂ and the third, in a subsequent photodimerization. By elemental analysis, the final amorphous solid product contains a C/Br atomic ratio >12, suggesting that Br₂ is acting photocatalytically. Even with a poorly optimized optical system, the reaction rate has reached as high as 1.6 mg reduced C with 40 s of solar collection using a 30 cm diameter paraboloid reflector. This rate is consistent with the storage of approximately 1% of incident solar energy.



Chlorophyll-containing cells are responsible for the bulk of solar-photochemical reduction of CO₂ to useful fuels and synthetic building blocks. Plants accomplish this CO₂ photo-reduction indirectly, by initially photoreducing H₂O and then using the product H₂ (or rather its biochemical equivalent) in the Calvin cycle to enzymatically reduce CO₂.

More direct solar photochemical reduction of CO₂ using catalytic photosensitizers has been investigated only in artificial systems based on transition-metal compounds.^{1–5} One class of reactions uses TiO₂ as both nanoparticle support and the photoelectron transfer agent to surface-bound CO₂.^{3–5} Recently, an organometallic sensitizer (a ruthenium-*bis*-pyridyl complex) and the enzyme carbon monoxide dehydrogenase have been chemically conjugated to such TiO₂ nanoparticles, permitting more efficient direct photoreduction of CO₂ to CO.⁵ One strategy that has been investigated as early as 1994 with such inorganic photosensitizers is to utilize compressed (supercritical or liquid) CO₂ as the reaction solvent, in order to take advantage of the resulting high reactant concentration to increase the rate of photoreduction.^{6,7} Other approaches for CO₂ reduction involve solar-powered or solar-assisted electrochemical cells.^{8,9} Here, we demonstrate a very different method of direct photochemical reduction of compressed CO₂, using simple elemental bromine as the photosensitizer.

MATERIALS AND METHODS

General Safety Note. Binary liquid solutions of CO₂ and Br₂ are easily prepared by combining liquid bromine and dry ice in a container, then sealing it tightly and allowing it to warm and pressurize. However, the resulting high pressures, approaching the 71 bar critical pressure of CO₂ as the temperature approaches *T*_c = 31 °C, substantially exceed the safety limits of the inexpensive silica and borosilicate containers

used for these experiments, and frequently resulted in explosions that sprayed glass fragments for many meters at high speeds. Damage from such explosions was mitigated by the careful use of small volumes, appropriate shielding, and geographic isolation.

Materials. Reagent grade Br₂ was from Aldrich. For some reactions, including all those used for mass spectrometry measurements, the Br₂ was distilled over concentrated H₂SO₄ prior to use. This eliminated sets of *m/z* peaks centered at 431 and 351, indicative of contaminant ions (likely PBr₅⁺ and PBr₄⁺, respectively).

Commercial dry ice (from Continental Carbonic Products, Inc.) was used without further purification. The specification sheet for this material indicates ~10 ppm of H₂O and CH₄ as contaminants; additional H₂O was likely introduced during the transfer of crushed dry ice into the reaction vessels. These minor contaminants clearly do not block the observed photoreactions. The lack of availability of purer CO₂ means it is still unknown whether these contaminants may actually be necessary for the reactions to occur.

Silica gel, 40–70 μm particle size, was from Sorbent. Powdered alumina was from Woelm. Titania, a generous gift from Dr. Tewodros Asefa, was originally from Degussa (grade P25). Glass wool was Corning type E fiberglass and was baked 30 min at 180 °C prior to use, in order to remove its hydrocarbon coating. Quartz wool was from Technical Glass (www.technicalglass.com).

Special Issue: Richard A. Mathies Festschrift

Received: September 16, 2011

Revised: December 23, 2011

Published: January 3, 2012

Reaction Vessels. Only custom made GL14-threaded fused-silica or borosilicate tubes with internal diameters under 1 cm were found to be suitable for containing the high pressures (10–75 bar) of CO₂ used for most of these experiments, in which high-pressure containment was required for hours or days. To make these containers, open-ended quartz and borosilicate tubes, with one end carrying a GL14 thread, were obtained from Technical Glass and ChemGlass, respectively. The unthreaded end was sealed by a professional glass blower (Ms. Sally Prasch), giving an overall tube length of ~10 cm. For some of the borosilicate reaction vessels, the GL14 thread was fused to a longer piece of larger-diameter thick-wall borosilicate tubing, to give a larger total volume. Closures used were red-colored GL14 caps with an inserted polytetrafluoroethylene (PTFE) seal, from ChemGlass. Seals were used only once; the red screw-cap closures themselves were reused. (Safety note: An alternative supplier's closures, although nearly identical in appearance, were found not to be sufficiently strong. They consistently failed, blowing out a disk of plastic with a small explosion when the liquid CO₂ reached temperatures near 0 °C, corresponding to pressures of 20–30 bar. However, such failures typically occurred with the ChemGlass GL14 caps only after many weeks of use.)

It was also found that commercially available conical-bottom microreaction vessels (specifically 1 mL Reacti-Vials from Pierce) were strong enough to hold liquid CO₂ samples. However, no closures available for these containers were found to be capable of sealing them for more than a few minutes at a time, when they contained a liquid CO₂ phase. Their thicker walls resulted in poorer focusing of sunlight onto the samples contained within them, and thus, such samples never produced more than small amounts of stable dark carbonaceous product from the solar photolysis reaction. Nevertheless, Reacti-Vials, along with solid plastic caps and PTFE-laminated silicone liners, were found to be suitable for carrying out small-volume photoreactions for producing small quantities of the transient red photoproduct, e.g., for mass spectrometry.

Prior to each use, photoreaction tubes were cleaned sequentially with detergent solution, water, and ethanol, and then dried. Polar adsorbent (0.1–1 g) was packed into the bottom of the photoreaction tube. Subsequently, the tube and its contents were dried at 80 °C for 2–48 h under a stream of dry air. (However, this thorough removal of water was sometimes eliminated, without noticeable effect on the results.) After cooling, CO₂ was added as dry ice, crushed in a polyethylene bag immediately prior to transfer into the reaction container so as to minimize formation of water frost on its surfaces. After this point, use of protective eye-ware was crucial at all times for all personnel near to the reaction container. Finally, a measured volume of Br₂ was added on top of the dry ice, using a glass micropipet.

Solar Illumination. Unless otherwise indicated, photoreactions were performed at 42.9549° N latitude, 75.8649° W longitude, at various times when the ambient temperature ranged from –20 to 30 °C and the solar elevation ranged from 20–70°. For initial small-scale experiments, sunlight was focused with a 45° off-axis paraboloid mirror, specifically, a condensing mirror that had been removed, along with its mount, from a detector port of a Nicolet 60SX infrared spectrometer. This mirror had a ~25 mm focal length and numerical aperture of ~0.6. Although theoretically capable of producing a focused solar spot size of 0.2 mm, observed spot sizes with this mirror were more typically ~1 mm.

For this small mirror especially, it was important to maintain a fixed focal point for the intense sunlight relative to the sample. With a stationary focusing optic, the focused image of the sun would be expected to be displaced by a distance equal to its diameter in as little as 2 min. Thus, a device for rotating the sample and focusing optic together, along an axis parallel to the Earth's rotation axis, was important for maintaining good focused solar intensity. This was accomplished by affixing the mirror and the sample holder to a hobbyist's telescope equatorial mount and tripod, obtained from Tasco (see Figure S-1, Supporting Information). This permitted tracking of the sun across the sky for periods of up to 20–30 min by adjustment of a single manual screw-knob on the equatorial mount.

Subsequently, for scale-up, larger reflective optics were used successfully, including 30 cm and 61 cm diameter paraboloid reflectors (Edmund Optics CS53-875 and CS53-876), with focal lengths of 7.62 and 15.24 cm, respectively. These nominally had somewhat larger numerical apertures than the small 45° reflector, but were not highly polished, and therefore typically produced spot sizes of 4–5 mm in diameter, i.e., considerably larger than indicated by their focal lengths (which corresponded to theoretical focused solar spot sizes of 0.6 and 1.2 mm, respectively). Sample holders were fashioned out of bicycle wheels that had nearly matching outer diameters for their rims, which could therefore be clamped concentrically onto the paraboloid reflectors. These larger cylindrically symmetric paraboloid reflectors were too heavy to mount on the equatorial telescope mount. However, their larger size and their symmetry facilitated pointing them accurately toward the sun while being hand-held. Optimum alignment was achieved by maximizing the solar intensity focused onto the bottom of the reaction tube. This was monitored by using a small hand-held inspection mirror, inserted between the bottom of the reaction vial, and the hole in the back end of the paraboloid reflector. The mirror apparatus was held in thick-rubber gloved hands, with a thick piece of Lexan used as a body and face shield to protect against explosions.

Inexpensive smaller commercially available paraboloid mirrors were also employed successfully. When these reflectors came in cylindrically symmetrical mounts, a simple plastic adaptor disk or bowl, that had had large portions of its off-axis area removed with a Dremel tool, could be taped concentrically onto them, in order to position a glass reaction vessel concentrically in them. This assembly was then easily propped up in a cylindrical vessel of about half the diameter of the reflector. This permitted stable pointing of the reflector assembly's axis toward the sun.

Electron Micrography. Scanning electron micrographs were obtained by Robert P. Smith at the SUNY-ESF electron microscope facility. Samples were placed directly on the grids and were sufficiently conductive that no deposition of a metal film (to prevent buildup of static charge) was necessary.

Mass Spectrometry. All mass spectrometry measurements were performed on a Thermo Polaris Q GC-MS instrument, (maintained and operated by David Kiemle, at the SUNY School of Environmental Science and Forestry). Small amounts of each sample were transferred on fragments of glass wool, from the photoreaction vessel, into the precooled solids probe of a GC-MS instrument, then allowing this sample to vaporize and ionize, while bypassing the gas chromatograph. Except as indicated below, measurements were performed with an initial temperature dwell of 3 min at 30 °C, followed by temperature

ramp of 50 °C per minute, to a final temperature of 350 °C for 3 min, before baking out the system for 10 min at 450 °C and cooling.

Mass spectral measurements of the transient red photoproduct formed in the initial phase of photoreaction of Br₂ with CO₂, was done without a programmed temperature ramp. The sample was freshly prepared immediately prior to the run, by packing ~0.01 g glass wool into the bottom of a 1 mL Pierce ReactiVial, then adding 5–10 µL freshly distilled Br₂ and ~0.5 g dry ice, capping it tightly with a solid screwcap and a PTFE-laminated silicone linear, and (within seconds) exposing it to the focused sunlight from a 15 cm diameter paraboloid mirror. (This was obtained from an after-market truck headlight, Rally Model 3125, purchased at a local auto parts store.) The solar illumination was performed at 43.0344° N latitude, 76.1376° W longitude, in a field just outside the laboratory building where the mass spectrometer is located. After ~30 s of illumination with focused sunlight, it was possible to visualize, with a small inspection mirror, that the dark-red transient photoproduct had collected on the glass wool at the bottom of the ReactiVial. This sample was cold-trapped by rapid release of CO₂ pressure, causing evaporation within ~1 s of the remaining 1–2 mL of liquid CO₂; followed by storage of the cold sample on dry ice for several minutes, while it was brought indoors to the mass spectrometer. The solids probe had been precooled to 0 °C. A few strands of glass wool from the reaction vial, still at dry ice temperature, were transferred to the probe by using precooled steel tweezers. Then, the probe was inserted into the mass spectrometer, and the measurement was begun, all within ~10 s of the sample transfer. Within several seconds, the probe warmed up to the lowest temperature setting possible (30 °C), and remained at that temperature throughout the run.

Density Functional Theory Computations. Energies of the individual molecules were computed, and geometries were optimized to a local energy minimum, by using GAUSSIAN03W (via GAUSSVIEW 4.1), with the following keywords: opt = tight b3lyp/6-311+g(2d,2p), integral = grid = ultrafine, scf = tight, symm = loose. The first of these specifies use of an extra-tight cutoff on forces and step size that are used to determine convergence during the optimization procedure, which is particularly useful for finding the optimum geometry in weakly bonded systems. The next keyword specifies a particular pairing of correlation and exchange functionals (B3LYP) and the orbital basis set used (6-311, supplemented with diffuse basis functions as well as polarization functions). The keyword beginning with “integral” requests a pruned computational grid that is finer than the default, having 99 radial shells and 590 angular points per shell, around each atom. The need to reach full (tight) convergence of the self-consistent field is specified by a subsequent keyword; this extra demand on the convergence goes hand-in-hand with adding diffuse basis functions. Finally, setting a loose constraint on the input symmetry forces the program to symmetrize crudely drawn molecular geometries before beginning the optimization procedures.

RESULTS

Our phenomenological observations of the bromine-sensitized CO₂ photolysis reaction confirm and extend those in a recently published provisional patent application.¹⁰ When sunlight is focused tightly upon a solution of Br₂ in CO₂, a smoke-like product rapidly evolves from the rapidly refluxing solution, and a grayish-white film deposits upon the container's inner

surfaces. This metastable film has not yet been amenable to analysis. However, when a polar adsorbent with closely apposed surfaces (powdered silica gel, alumina, or titania; or quartz or glass wool) is additionally present at the point of illumination, metastable intermediates are evidently concentrated for long enough to permit their further photochemical reaction. The end product is a dark solid film that forms on the surface of the polar adsorbent (see Figure 1) and which remains visible after the pressure is released and excess Br₂ evaporates.



Figure 1. Multiple dark spots are visible where focused sunlight produced the stable carbonaceous product of bromine-sensitized photolysis of CO₂. The sample is pressurized to ~60 bar; the orange-colored phase is 0.5% Br₂ in liquid CO₂. The meniscus between this liquid and the gaseous phase (not shown) sits just above the top edge of the photograph. Separate 1 mm sized black spots on the powdered-alumina bed represent distinct 20 s intervals of illumination spread over 2 successive midday periods, with the sample recooled to –20 °C and repositioned in between each interval. The bottom half of the 90° off-axis paraboloid mirror is visible at the top of the image, behind the sample holder.

The highest rates of formation of this dark stable photoproduct were obtained with a reactant bulk temperature of 0–20 °C, using tightly packed glass or quartz wool as the polar adsorbent, and a Br₂ concentration of ~0.5% in liquid CO₂. Besides providing the highest possible concentration of the CO₂ reactant, an advantage of using a bulk liquid CO₂ phase is the efficient cooling available from its refluxing while boiling in the optimum temperature range. However, with low initial temperatures, small reaction volumes, and correspondingly small focusing mirrors to keep the temperature from rising too quickly, the stable photoproduct can be produced using supercritical CO₂ or even with a total amount of CO₂ as small as 20 mg per mL of reaction volume. The latter conditions correspond to a pressure of only ~10 bar at 0 °C and a fairly low concentration of dissolved CO₂ in the liquid Br₂.

Formation of the stable dark photoproduct occurs only after a lag period of ~1–20 s following initiation of illumination with tightly focused sunlight. During this period, a viscous ruby-red

liquid can be observed to form a separate phase and to accumulate near the illuminated spot, while the orange color of the bulk liquid CO_2 solution is visibly depleted. In addition to this red intermediate, a subsequent transient intermediate can often be observed, with distinctive white luminescence.

If illumination is interrupted prior to deposition of the dark product, the red intermediate visibly decays, with a lifetime of ~ 10 s near 20°C , accompanied by restoration of the initial orange-colored solution. The red photointermediate can also be produced by focusing 0.5 W of 457 nm light from an Ar^+ laser (but not other laser lines of 488 or 514 nm, which are not within the absorption band of Br_2) onto a sample consisting of tightly packed glass wool in a liquid phase consisting of 1% Br_2 in CO_2 , at 0°C . Under such conditions, the transient red photoproduct streams slowly downward from the point of illumination, indicating that it is denser than the bulk liquid CO_2 .

In contrast, no duration of 457 nm laser illumination has sufficed to produce the luminescent intermediate, nor the stable dark end product. UV light appears to be required for these further photoreactions to occur. Attenuating the UV component of sunlight also blocks them, while still allowing production of the red metastable intermediate. The observed photoreactions also have an absolute requirement for Br_2 . Other inexpensive photosensitizers that failed to show any similar photosensitized reactions include titania, hemin, and carbon (e.g., graphite powder or candle soot).

Analysis of the Stable Product(s). Samples photolyzed using glass wool as the polar adsorbent gave the highest rates of formation of reduced carbon. Elemental analysis indicated a maximum incorporation of 4% combustible carbon in the blackened region of the glass-wool substrate (corresponding to a total of 1.6 mg of reduced carbon in a 41 mg sample sent for analysis). This was obtained from a sample originally containing 4 g of CO_2 , 0.1 g of type E fiberglass, and 0.016 g of Br_2 . Assuming that the enthalpy of this combustible-carbon product was similar to that of elemental carbon, the energy storage was 52 J, or about 1.3% of the total solar energy collected. (This total energy was 3.8 kJ, based on the 40 s illumination period, the collection area of 0.07 m^2 , and the solar constant of 1366 W/m^2 .)

The chemical state of the carbon in the product has not been fully elucidated, but elemental analysis showed it contained roughly half as much Br as C by weight. The corresponding large C/Br atomic ratio of 13:1 suggests that the Br_2 is acting at least partially photocatalytically. The presence of Br in the product does not alter the estimate of energy storage since the enthalpy of formation of bromocarbon compounds (from graphite and Br_2) is always positive (but small). However, the energy storage could be significantly overestimated if the product still contained a significant amount of oxygen, i.e., if the carbon were only partially reduced.

To date, we have not been able to determine the O content of the stable end product, due to an inability to separate it from the polar substrate on which it formed. The best separation was obtained when the reaction was carried out using pure silica materials for the polar substrate. Either silica gel or quartz wool used in this manner could be largely digested and dissolved by treatment for 1–3 days in 10 M NaOH at 80°C , followed by extensive washes of the black residue in water, with centrifugations in between. However, even this extensively digested material gave at most 12% carbon upon combustion analysis, suggesting that the carbonaceous product was capable

of protecting a significant portion of the silica substrate from chemical attack by alkali.

Scanning electron microscopy (SEM) of the carbonaceous product on the glass-wool polar substrate indicated mainly amorphous islands $\sim 1\text{ }\mu\text{m}$ in dimension, with a few longer tubular structures admixed (see Figure 2). The alkaline

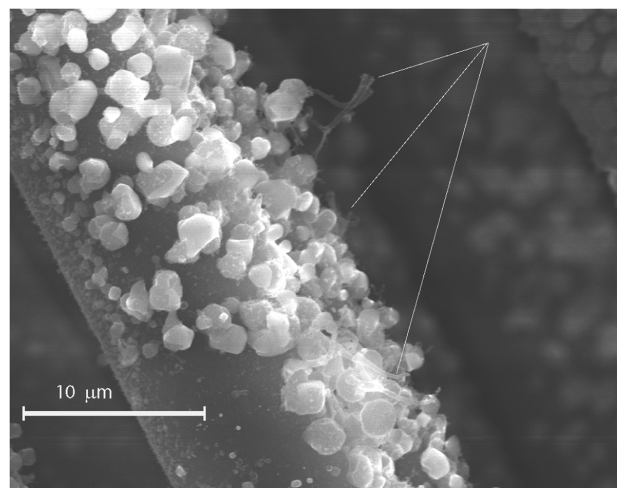


Figure 2. SEM of the stable carbonaceous product of $\text{CO}_2 + \text{Br}_2$ photolysis, obtained using fiberglass (Corning Type E, laboratory glass wool) as the polar substrate. The 3 lines point to examples of tubular structures, spread among the predominantly amorphous particles deposited on the fiber surfaces. This image was obtained using 30.0 kV, 3700 \times magnification, 0 tilt, and $0.034\text{ }\mu\text{m}$ per pixel.

digestion process, when applied to a sample prepared using silica gel as the polar substrate, apparently selected for the largest particles in the sample, yielding $\sim 100\text{ }\mu\text{m}$ clumps composed of $10\text{ }\mu\text{m}$ particles (see Supporting Information).

Mass spectrometry of the condensed-phase products gave no indication of formation of elemental carbon, e.g., fullerenes, with m/z at some multiple of 12. Small amounts of volatile perbrominated hydrocarbons were likely formed, e.g., C_2Br_4 as indicated by a set of m/z peaks at 340, 342, 344, 346, and 348 (see Supporting Information). Additional less volatile non-brominated products were also formed; these exhibited a characteristic set of m/z peaks at 217, 183, 176, 91, 86, and 65 that were detected only when the mass spec solid probe reached $\sim 350^\circ\text{C}$. Our observations do not yet permit identification of the corresponding chemical formula(s).

Identity of the Metastable Red Intermediate. Mass spectrometry of the cold-trapped red species yielded m/z peaks at 406, 408, 410, 412, and 414 in the natural-abundance isotope ratio expected for a tetrabromo species, specifically for a molecular ion with the formula $\text{C}_2\text{O}_4\text{Br}_4^+$ (see Figure 3). These 5 peaks all decayed rapidly, within ~ 40 s, much faster than the residual Br_2 reactant (see Figure 3, inset). Additional peaks that decayed on the same time scale corresponded to the same species with a methyl group (15 mass units) added, possibly arising due to a small methane contaminant in the dry ice used for the photoreaction. Other prominent sets of peaks in Figure 3, centered near 330 and 345, correspond, respectively, to the species centered near 410 and 425, each minus a Br atom. No m/z peaks were observed corresponding to direct adducts of Br_2 to a single CO_2 molecule, e.g., CO_2Br_2 ($m/z \approx 204$) or CO_2Br_4 ($m/z \approx 364$).

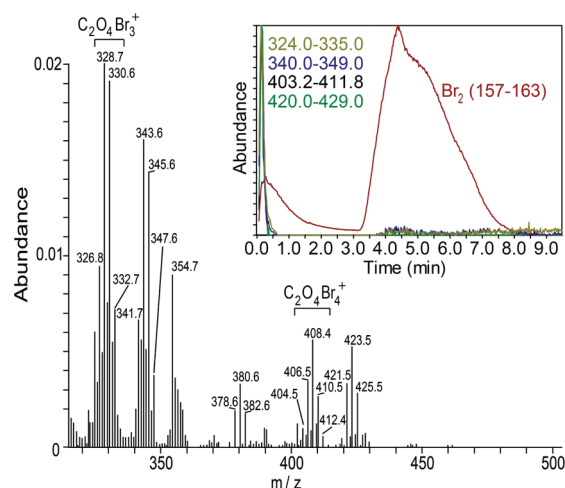
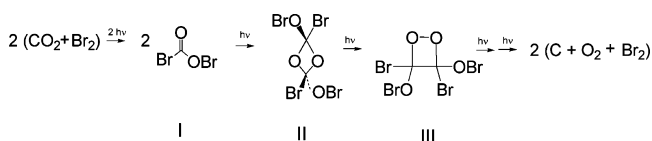


Figure 3. Mass spectrum from metastable photoproduct(s) of $CO_2 + Br_2$, measured during the first 50 s after transferring the cold-trapped reaction products into the mass spectrometer. The y axis is normalized to the m/z peak at 160 from $(^{79}Br^{81}Br)^+$, the molecular ion of the major isotopomer of residual Br_2 . Inset, comparison of four nearly superimposable time courses of detected ions (integrated ranges of 324–335, 340–349, 403–412, and 420–429) with the much different time course of Br_2 at m/z = 158–162. Each time course is rescaled by normalizing to its maximum value during the 9 min time of measurement.

Further analyses on the transient red photoproduct have not so far been attempted. However, its deep red color matches that reported for known alkyl hypobromites.^{11–13} Acyl hypobromites, however, have been reported to have a strong green color,¹⁴ although, as with the alkyl hypobromites,¹⁵ this color results only from the long-wavelength tail of a broad absorption band that reaches its maximum in the UV. Nevertheless, in conjunction with the mass spectrometry, the color of the transient red species helps to rule out bromoformyl hypobromite (I in Scheme 1) as its structure.

Scheme 1



It is nevertheless reasonable that CO_2Br_2 should be the primary photoproduct of Br_2 in CO_2 solution. This hypothesis is supported by the stability of the fluorine analogue of I, fluoroformyl hypofluorite, although the latter has been produced only by photochemical reaction of F_2 with bis-(fluoroformyl) peroxide, rather than with CO_2 .¹⁶ If trapped at a polar surface in high concentration, I might well be expected to photodimerize to a kinetically more stable $C_2O_4Br_4$ species (II or III), as suggested in Scheme 1.

We have performed density functional theory (DFT) computations, indicating that I has an energy 207 kJ mol^{-1} above $(CO_2 + Br_2)$. This is somewhat less than the 260 kJ mol^{-1} available from blue (450 nm) photons. DFT computations also indicate that the lowest energy isomer of $C_2O_4Br_4$ is *trans*-2,4-dibromo-2,4-dihypobromo-1,3-dioxetane (II). Its energy is $\sim 130 \text{ kJ mol}^{-1}$ above that of a pair of bromoformyl hypobromite (I) molecules. (The *cis* form of II is

computed to be $\sim 1 \text{ kJ mol}^{-1}$ higher in energy than that of the *trans*; see Supporting Information.) In contrast, the next lowest energy $C_2O_4Br_4$ isomer, 3,4-dibromo-3,4-dihypobromo-1,2-dioxetane, III, is computed to be $\sim 400 \text{ kJ mol}^{-1}$ above two molecules of I. That is, photodimerization of I to II could be accomplished with the energy of a single visible photon, while photodimerization of I to III would require at least two, as suggested by Scheme 1.

Another isomer of $C_2O_4Br_4$, tetra(hypobromyl)ethylene, gives a computed energy of $\sim 320 \text{ kJ mol}^{-1}$ above two molecules of I, and an optimized geometry that is far from symmetrical: two of the four O–Br bonds are $>2.5 \text{ \AA}$ in length, meaning that the structure is essentially two Br atoms plus di(hypobromyl) oxalate, $C_2O_4Br_2$. This isomer can thus be ruled out as the structure for the red transient photoproduct.

DISCUSSION

Br_2 and CO_2 were both first isolated in condensed phases in 1825, and their gas phase binary combination has been used for decades, e.g., as a chemical oxidant¹⁷ and in flashlamp-pumped lasers.¹⁸ Despite this long history, no photochemical or thermal reactivity between Br_2 and CO_2 has previously been noted. This is likely because their photoreaction rate to form a metastable adduct depends supralinearly on both photon and CO_2 concentrations. Unpressurized CO_2 at ambient temperatures and unfocused sunlight are simply too dilute to observe any reaction products

Additionally, the formation of the metastable adduct evidently depends on interactions between the fluid phase reactants and a polar adsorbent material. The latter can be considered as a form of requisite heterogeneous catalyst. However, quite a variety of polar materials that can be used, including oxides of silicon, aluminum, and titanium. The looseness of this structural requirement, as well as the chemical stability of these materials and their high electronic bandgaps, suggest that such catalysts are not serving as accessory photosensitizers; nor directly donating or accepting any electrons. We hypothesize instead that their role may be to concentrate transiently formed polar monomers (I) between closely apposed adsorbent surfaces, positioning these monomers for photodimerization to a metastable intermediate (e.g., II), and for further photoreaction(s) to give stable end products.

The dark stable photoproduct contains combustible carbon. It must therefore have an O/C ratio of less than 2:1. Among stable carbon compounds, only carbonates (and CO_2 itself) have $O/C \geq 2$, and these would not be detectable by combustion analysis. By simple algebra and conservation of atoms, there must be concomitant formation of an oxidized species, with O/C atomic ratio greater than the value of 2:1 present in the initial CO_2 reactant.

We have not yet made any effort to directly detect the presumed oxidized photoproduct, O_2 . Nevertheless, it is a nearly inescapable conclusion that O_2 must also be produced by the observed photoreaction. Besides O_2 , the most obvious possible oxidized products with suitable O/C ratios are O_3 and bromine oxides. However, even the most stable of these (Br_2O) would be expected to decompose to form O_2 quite rapidly under our reaction conditions.¹⁹ It is impossible to rule out more exotic oxidized photoproducts such as organic polyhypobromites, e.g. $C(OBr)_4$ or $C_2(OBr)_6$. However, such compounds have never been reported, are not detectable by mass spectrometry in the final products, and are computed to

have very high energies (see Supporting Information). This suggests that they would likely decompose to give O₂ by spontaneous decomposition at ambient temperatures, even if they are formed even transiently. An alternative possibility that the polar substance needed for this photoreaction (silica or alumina) undergoes oxidation is also unlikely because stable higher oxidation states of silicon and aluminum are unknown.

The principal conclusion of this work is that the most likely structure for the metastable red photoproduct is structure **II** in Scheme 1. However, this species does not contain reduced carbon. The mechanism of the subsequent photoreduction process is murky. Formation of **III** from **II** in Scheme 1 would accomplish the formation of C–C and O–O covalent bonds, both of which appear to be crucial for the overall photoreduction process. However, there is a great variety of other possible photoproducts of **II** whose energies have not been exhaustively computed; a number of these also contain C–C and/or O–O bonds. Thus, inclusion of the photoreaction from **II** to **III** in Scheme 1 is presented only as an interesting speculative possibility, i.e., with much less confidence than the formation of **II** itself.

Our inexpensive optical systems give an intensity only 10³–10⁴ times unfocused sunlight, several orders of magnitude less than theoretically possible. Nevertheless, the specific photocatalytic turnover obtained, 1.6 mg reduced C from 16 mg Br₂ with 40 s illumination or 6000 mg C per g of photosensitizer per hour, is already 600 times one of the best previously reported values, ~10 mg of reduced CO₂ per gram of TiO₂ photocatalyst per hour.⁵ Solar energy storage efficiencies obtained so far from the bromine-sensitized photolysis process (~1%) are considerably lower than from silicon photocells, the best of which now exceed 50%. With optical optimization, however, the efficiency could conceivably become competitive.

Raw material cost may be an even more impressive measure of potential economic efficiency. In comparison to heavy metals such as Ru or Co, whose compounds are often used for photosensitizing CO₂, the crustal abundance of Br is at least 1000-fold greater. The cost of elemental Br₂ is correspondingly low, in U.S. dollars, \$1.50 per kg in bulk, which is even less than bulk TiO₂, and nearly as inexpensive as elemental Si. However, this low cost of photosensitizer material must be weighed against capital costs of the requisite optical focusing apparatus, of transparent vessels capable of holding high pressures, and of cooling systems; as well as the cost of capturing and recycling excess Br₂ and volatile bromocarbon compounds that are formed as byproducts. Nevertheless, with further long term development, this process could conceivably become a useful method for chemically sequestering CO₂ and/or for solar-powered fuel synthesis.

There may also be a potential for performing other new types of green chemistry with the newly prepared molecule C₂O₄Br₄, besides converting it to fuels. This species, whose lowest-energy isomers are computed to store at least half as much energy per carbon atom as coal, can be synthesized quickly by using solar energy and cold-trapped as a supercooled liquid. Its tandem hypobromite groups are likely to have specific reactivities beyond those of simpler alkyl hypobromites,¹² thereby making this molecule useful in the synthesis of fine chemicals.

We propose that the metastable red photoproduct is specifically a dibromo dihypobromo dioxetane, most likely a 1,3-dioxetane (**II**). This species has a computed energy that exceeds that of the starting materials (CO₂ and Br₂) by an amount that is 2/3 as big as the value expected if the CO₂ were

to be decomposed into its elements. (The latter value was not computed but was obtained from the well-known experimental value of –400 kJ mol^{–1} for the combustion enthalpy of graphite.) Thus, the energy required for **III** to be further photoreacted to its elements is (just barely) available from a single additional blue photon. However, there are no clear precedents in the literature for photochemical or thermal decomposition of dioxetanes via C–O (rather than O–O) bond scission. Therefore, none of the possible pathways for molecule **II** (and/or **III**) to photoreact to form reduced-carbon species can yet be considered as more than speculation.

■ ASSOCIATED CONTENT

● Supporting Information

Details of the methods used to produce samples for elemental analysis, including photographic images of the samples in their reaction tubes; a photographic image of the transient red species; the full range (50–500 amu) of its mass spectrum is shown in Figure 3, along with a control unilluminated sample; mass spectra of some of the stable photoproducts; and a table of DFT-optimized geometries (Z-matrices) and computed energies of CO₂, Br₂, and several geometric isomers of species **I**, **II**, and **III** in Scheme 1. This material is available free of charge via the Internet at <http://pubs.acs.org>.

■ AUTHOR INFORMATION

Corresponding Author

*E-mail: mbrainan@syr.edu.

■ ACKNOWLEDGMENTS

This work was supported by 4Thought Technologies and by Syracuse University. W.S.K. was supported by an NSF iRES grant for undergraduate summer research. We thank Damian Allis for advice in performing computations; Sally Prasch for fabricating glass containers capable of holding unusually high pressures; David Kiemle for mass spectrometry, Robert Smith for electron micrography, and Tewodros Asefa for providing samples of nanostructured titania. We also thank Bruce Hudson, John Baldwin, Joseph Chaiken, Don Dittmer, and Jon Zubietta for useful advice on interpretation. M.S.B. would like to express appreciation to Rich Mathies who taught him, through example and encouragement, the value of fearlessness in scientific research.

■ REFERENCES

- (1) Morris, A. J.; Meyer, G. J.; Fujita, E. Molecular Approaches to the Photocatalytic Reduction of Carbon Dioxide for Solar Fuels. *Acc. Chem. Res.* **2009**, *42*, 1983–1994.
- (2) Hoffmann, M. R.; Moss, J. A.; Baum, M. M. Artificial Photosynthesis: Semiconductor Photocatalytic Fixation of CO₂ to Afford Higher Organic Compounds. *Dalton Trans.* **2011**, *40*, 5151.
- (3) Somnath, C. R.; Varghese, O. K.; Paulose, M.; Grimes, C. A. Toward Solar Fuels: Photocatalytic Conversion of Carbon Dioxide to Hydrocarbons. *ACS Nano* **2010**, *4*, 1259–1278.
- (4) Kuwabata, S.; Uchida, H.; Ogawa, A.; Hirao, S.; Yoneyama, H. Selective Photoreduction of Carbon Dioxide to Methanol on Titanium Dioxide Photocatalysts in Polypropylene Carbonate Solution. *J. Chem. Soc. Chem. Commun.* **1995**, 829–830.
- (5) Woolerton, T. W.; Sheard, S.; Reisner, E.; Pierce, E.; Ragsdale, S. W.; Armstrong, F. A. Efficient and Clean Photoreduction of CO₂ to CO by Enzyme-Modified TiO₂ Nanoparticles Using Visible Light. *J. Am. Chem. Soc.* **2010**, *132*, 2132–2133.

- (6) Mizuno, T.; Tsutsumi, H.; Ohta, K.; Saji, A.; Noda, H. Photocatalytic Reduction of CO₂ with Dispersed TiO₂/Cu Powder Mixtures in Supercritical CO₂. *Chem. Lett.* **1994**, 23, 1533.
- (7) Grills, D. C.; Fujita, E. New Directions for the Photocatalytic Reduction of CO₂: Supramolecular, scCO₂ or Biphasic Ionic Liquid-scCO₂ Systems. *J. Phys. Chem. Lett.* **2010**, 1, 2709–2718.
- (8) Licht, S.; Wang, B.; Ghosh, S.; Ayub, H.; Jiang, D.; Ginley, J. A New Carbon Capture Process: Solar Thermal Electrochemical Photo (STEP) Carbon Capture. *J. Phys. Chem. Lett.* **2010**, 1, 2363–2368.
- (9) Cole, E. B.; Lakkaraju, P. S.; Rampulla, D. M.; Morris, A. J.; Abelev, E.; Bocarsly, A. B. Using a One-Electron Shuttle for the Multielectron Reduction of CO₂ to Methanol: Kinetic, Mechanistic, and Structural Insights. *J. Am. Chem. Soc.* **2010**, 132, 11539–11551.
- (10) Braiman, M. Bromine-sensitized Solar Photolysis of Liquid CO₂. U.S. Patent 61,313,740, Sept 14, 2011.
- (11) Bushong, F. W. On the Alkyl Hypobromites, R–O–Br. *Transactions of the Kansas Academy of Science*, **1896**, 15, 81–82.
- (12) Walling, C.; Pawda, A. Positive Halogen Compounds. V. *t*-Butyl Hypobromite and Two New Techniques for Hydrocarbon Bromination. *J. Org. Chem.* **1962**, 27, 2976–2978.
- (13) Roscher, N. M.; Nguyen, C. K. Spectrophotometric and Titrimetric Studies on Alkyl Hypobromites. *J. Org. Chem.* **1985**, 50, 716–717.
- (14) Reilly, J. J.; Duncan, D. J.; Wunz, T. P.; Patsiga, R. A. Isolation and Properties of Acetyl Hypobromite. *J. Org. Chem.* **1974**, 39, 3291–3292.
- (15) Anbar, M.; Dostrovsky, I. Ultra-violet Absorption Spectra of Some Organic Hypohalites. *J. Chem. Soc.* **1954**, 1105–1108.
- (16) Argüello, G. A.; Balzer-Jöllenbeck, G.; Jülicher, B.; Willner, H. Properties of Fluoroformyl Hypofluorite, FC(O)OF, Revisited. *Inorg. Chem.* **1995**, 34, 603–606.
- (17) Yamauchi, S.; Mukaibo, T.; Hirano, M. Effect of Bromine on the Oxidation of Graphite by Carbon Dioxide. *Carbon* **1967**, 5, 243–245.
- (18) Peterson, B.; Wittig, C.; Leone, S. R. Infrared Molecular Lasers Pumped by Electronic-Vibrational Energy Transfer from Br(4²P_{1/2}): CO₂, N₂O, HCN, and C₂H₂. *Appl. Phys. Lett.* **1975**, 27, 305–307.
- (19) Seppelt, K. Bromine Oxides. *Acc. Chem. Res.* **1997**, 30, 111–113.